Mpemba-Like Behavior in Carbon Nanotube Resonators

P. ALEX GREANEY, GIOVANNA LANI, GIANCARLO CICERO, and JEFFREY C. GROSSMAN

Surprising Mpemba-like dissipation is observed during computer simulated ring-down of the flexural modes of a single-walled carbon nanotube resonator. Vibrations are made to decay to zero faster by adding a *larger* initial excitation. We liken this counterintuitive observation to the well-known Mpemba effect in which hot water freezes faster that cold water. In both cases, the system seems to pose a memory of its thermal history; a paradoxical result that is reconciled if the dissipative state of the system is not described uniquely by the system's average temperature. A vibrational mode projection algorithm is used to track the dissipation pathway, showing that dissipation is dependent strongly on the development of an athermal phonon population. The implications of Mpemba-like behavior in more general, and continuously driven, nanomechanical systems are discussed.

DOI: 10.1007/s11661-011-0843-4

I. INTRODUCTION

CARBON nanotubes (CNTs) posess several properties that make them attractive for use as resonating members in many nanoscale devices. The use of CNT resonators has already been demonstrated as a radio tuner,[1] an entire radio receiver,[2] and a radio transmitter.[3] In addition, CNT resonators have been used to measure minuscule masses,[4] even down to the mass of a single Au atom,[5] and to approach the quantum limits of vibration.[6] In addition to these demonstrated applications, the potential uses for CNT resonators are much broader, being applicable to any nanoscale device that requires controlled vibration, such as gyroscopes, mechanical processing of signals, and simple mechanical time keeping. The reasons why CNTs are so suitable are multifold: The extraordinarily high stiffness of CNTs combined with their low density enables them to attain high natural frequencies and frequency sensitivity. That CNTs are quasi one-dimensional or string like provides well-defined strategies for tuning their frequency—for example, one may alter their length or put them under tension. Finally, CNTs can be both driven, and sensed, electronically by several different methods, which makes it possible to integrate CNTs into more complex nanoelectromechanical systems (NEMS) in which the resonator is only one part of the device.

To date, the biggest impediment to the use of CNTs as resonators is their poor quality factor Q, which when measured at ambient temperatures (and under conditions of constant driving) falls in the range of 8–300. (Q is defined to be 2π times the inverse fraction of oscillator energy lost per cycle, and it may be thought of as roughly the number of oscillations it takes for the energy to reduced by 99.8 pct.) This result has been resistant to improvement, having been observed both under vacuum and at ambient pressure; in both cantilevered and doubly clamped geometries with many different clamping methods; and through many different measurement techniques.[4,7–10] Only recently by cooling to milikelvin temperatures have Qs in excess of 10^5 been attained.[11] The universally poor ambient temperature results suggest that an intrinsic damping mechanism may be dominant. Roukes and colleagues,[12,13] and others[14] suggested that the intrinsic thermoelastic damping mechanism can produce low Q factors in CNTs because of their small surface-to-volume ratio. Previous computational work by Jiang *et al.*,[15] of an open-ended, cantilevered CNT found $Q = 1500$ at 293 K (20 °C), with the unexpected temperature dependence: $Q \sim T^{-0.36}$, although the authors did not identify an intrinsic damping mechanism explicitly.

II. METHOD

The motivation of this work is to simulate the simplest system possible with the aim of isolating and identifying only intrinsic damping mechanisms and to study the detailed pathway of dissipation with the goal of developing informed strategies for improving the Q factor of real systems. To this end, classical molecular dynamics simulations were performed of the ring-down of CNT flexural modes in a vacuum. The tubes were unclamped to remove associated extrinsic damping sources, but a clamping of sorts was applied by the use of periodic boundary conditions that restricted the

P. ALEX GREANEY, Postdoctoral Researcher, and JEFFREY C. GROSSMAN, Professor, are with the Department of Materials Science and Engineering, Massachusetts Institute of Technology, Cambridge, MA 02139. Contact e-mail: jcg@mit.edu GIOVANNA LANI, PhD Student, is with the Laboratoire des Solides Irradis, Ecole Polytechnique, 91128 Palaiseau Cedex, France. GIANCARLO CICERO, Professor, is with INFM and Physics Department, Polytechnic of Torino, I-10129 Torino, Italy.
Manuscript submitted March 21, 2010.

Published online: 16 August 2011

number and wavelength of the CNT's flexural modes*.

*The frequencies of flexural modes in the unclamped tube are higher than the modes of the same wavelength in the doubly clamped counterpart as there is no center of mass motion.

A typical simulation proceeded as follows:

(a) The CNT structure is relaxed, and the periodic repeat distance optimized.
(b) The stiffness matrix for the system is computed and then diagonalized to yield the tube's eigenmodes, and their frequencies.
(c) The tube is heated to a desired background temperature T_{bg} and allowed to equilibriate.
(d) An instantaneous velocity is added to the system along *one* particular eigendirection (usually that of the second flexural mode) such that the total *average* temperature of the system is raised by the amount T_{ex}.
(e) Ring-down is simulated in the microcanonical ensemble during which the vibrational energy distribution in all of the modes of the CNT is tracked using a projection algorithm.[16]

In all cases, the carbon–carbon interactions were modeled using the adaptive-intermolecular reaction empirical bond order (AIREBO) potential[17] implemented in the LAMMPS simulation package (Sandia Corporation, Albuqherque NM).[18] Trajectories were integrated using the velocity Verlet scheme with a 0.2-fs time step that minimized fluctuations in the total energy to less than 10^{-6} of the total thermal energy. The excitations of the flexural mode were large; however, despite the energetic excitations, it was found that the mode remained reasonably harmonic, containing at most a 5 pct anharmonic contribution to the potential energy.

In this work, we relied extensively on computational "experiments" to investigate dissipation mechanisms. It is therefore imperative to ensure that the computational methods used are meaningful. The dissipation phenomena studied arise only because of anharmonic interactions. Although the parametrization of the AIREBO potential has been fit to interactions of sp^2 and sp^3 bonded hydrocarbons, it has not been fit explicitly to the anharmonic properties. Thus, it was necessary to verify the robustness of the reported simulation results to changes in interatomic potential, for example, by simulating with and without Lennard-Jones and/or the torsional interactions turned on. Whereas the results of the simulations *are* found to be sensitive to changes in the interatomic potential, the overall qualitative behavior is not. This may be in part because the dissipative behavior is a result of the shapes of the low-frequency modes, which are dictated largely by the tubular geometry rather than the details of the potential. We observed also the Mpemba-like behavior to occur in CNTs of differing length, aspect ratio, and chirality (although the flexural modes of chiral tubes are slightly different and are corkscrew shaped). In these cases, the details of the dissipation differs but the same qualitative effect is observed. Supporting our assertion that the effect is geometric in origin, we do not observe Mpemba-like dissipation in graphene resonators of equivalent size.

It should be noted the simulations were performed using classic molecular dynamics at temperatures *below* the Debye temperature for the CNT. This is justified *a posteriori* by the finding that low-frequency modes participate in the dissipation mechanism. Leaving aside the issue of mode occupancy, a more fundamental problem is the use of classic mechanics to simulate the dissipation of an energy that is quantized. Unfortunately, as a more suitable method that includes quantized dynamics is lacking, we use classic dynamics with the understanding that the physical interpretation of our results is limited.

III. MPEMBA-LIKE BEHAVIOR

The ring-down curves for the second flexural mode of a 8.4-nm long (10,0) CNT, with a background temperature of T_{bg} = 5 K (−268 °C), and with increasing levels of initial excitation are shown in Figure 1(a). The data for each curve are the average of 10 separate simulations with differing initial conditions; the data are plotted with a broad line thickness chosen such that it encloses the deviation of the averaged data. It can be observed that the attenuation of the oscillation follows a sigmoidal path, with larger initial excitations being damped completely in a shorter time than softer excitations. Figure 1(b) shows the ring-down profile for a 150 K (−123 °C) excitation in tubes with increasing thermal background. As the background temperature increases the region of fastest attenuation is moved to earlier times.

A consequence of simulating in the microcanonical ensemble is that the CNT is a closed system; energy dissipated from the excited flexural mode accumulates in the rest of the vibrational modes of the tube, raising T_{bg}. Increasing T_{ex} independently from T_{bg} changes the average temperature of the system, and thus, one would expect a different attenuation profile. More remarkable is the cooling of the excited mode in systems in with the same total energy, $T_t = T_{bg} + T_{ex}$, but differing *initial* partitioning of this energy between the flexural mode and the background (shown in Figure 1(c)). Starting a simulation further from equilibrium (that is with larger initial T_{ex}/T_{bg}) causes the system to reach equilibrium in a faster time! We refer to this astounding, and counter-intuitive behavior, as "Mpemba-like" in analogy with the Mpemba effect[19] in which it is observed that hot water freezes faster than cold water. Figure 1(d) shows the ring-down time for increasing initial T_{ex} in systems for which $T_{ex} + T_{bg}$ = 300 K (27 °C). Two measures of the ring-down time are plotted: The time taken for excitation to be damped to a fixed lower threshold, and the interval over which the excitation is diminished by a set fraction—both measures decrease the further one starts from equilibrium. Like with the Mpemba effect, relaxing faster to equilibrium the further one starts from it can only occur if the cooling pathway is not unique, but instead depends on the system's initial

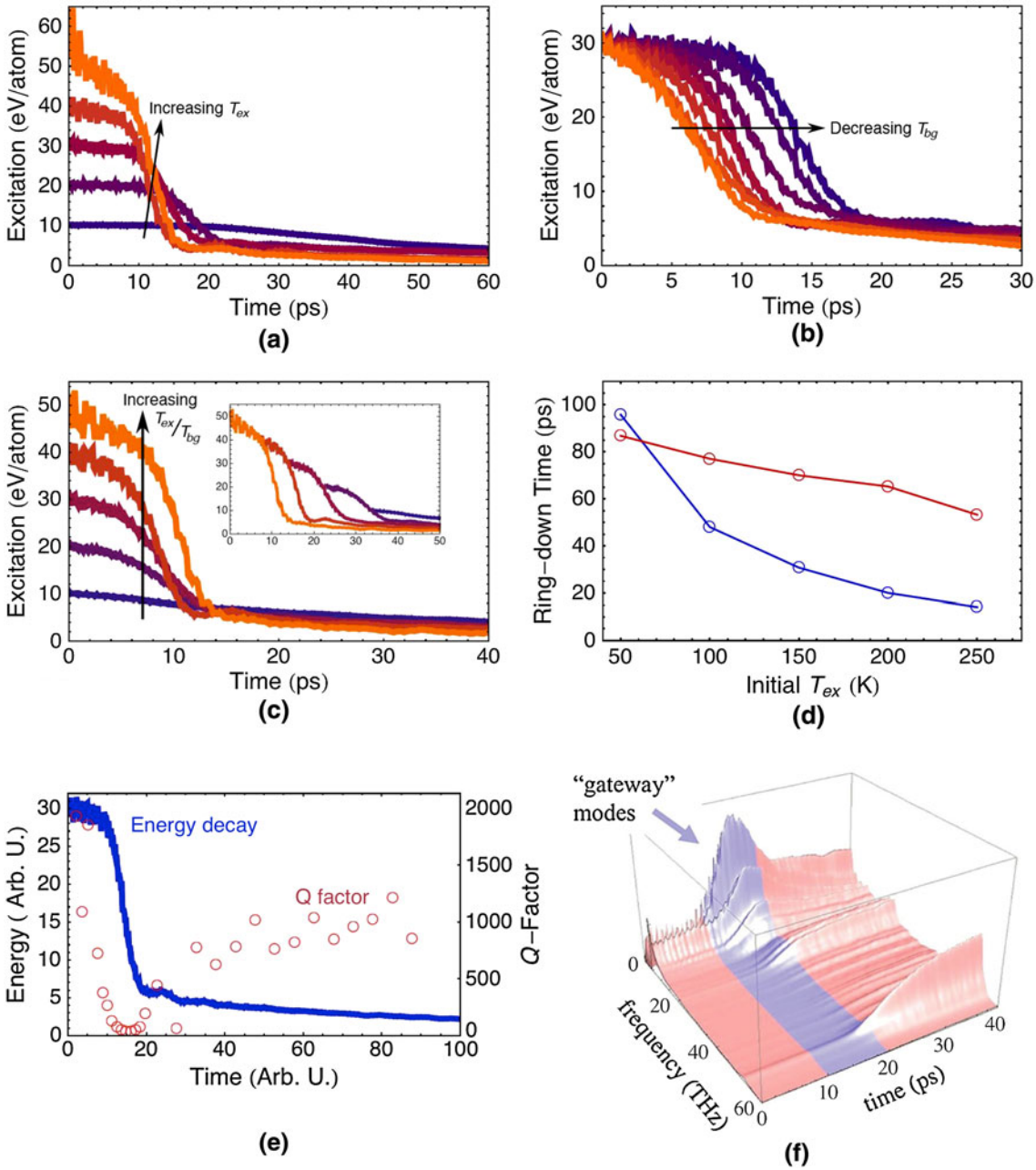

Fig. 1—Ring-down profiles for the second flexural modes in 8.4-nm long (10,0) CNTs. In all cases, the data are the average of 10 simulations. Plot (*a*) shows tubes with initial T_{bg} = 5 K and T_{ex} = 50 K, 100 K, 150 K, 200 K, and 300 K (−223 °C, −173 °C, −123 °C, −73 °C, and 27 °C), with the plotting colors getting progressively warmer from dark blue to orange as T_{ex} increases. Plot (*b*) shows the attenuation profile in tubes with initial T_{ex} = 150 K (−123 K), and T_{bg} = 5 K, 10 K, 50, K 100 K, 150 K, 200 K, 400 K, and 400 K (−268 °C, −263 °C, −223 °C, −173 °C, −123 °C, −73 K, 127 °C, and 127 °C). Plot (*c*) shows the total ring-down profiles for the simulations in which the total energy T_{bg} + T_{ex} = 300 K but with different initial partitioning ratios, T_{ex}/T_{bg}, between the excited and the background modes. As with the Mpemba effect, the mode cools faster if it begins at a hotter temperature. The inset plot shows the same cooling curves translated in time so that the more weakly excited simulations commence on the cooling path for more strongly excited simulations. It can be observed clearly that the curves do not lie on top of each other and there is not a universal cooling trajectory. The total ring-down time for these simulations are shown in plot (d), with the red line the time taken for the excited mode to decay to and excitation of 1.5 eV/atom, and the blue plot the time taken for the mode to lose 88pct of its initial energy. Plot (e) shows the ring-down for initial T_{bg} = 5 K, T_{ex} = 150 K (−123 °C) (blue) plotted in conjunction with the *Q* factor (red circles). The surface plot (f) shows how the dissipated energy from this simulation is distributed over the spectrum of CNTs background vibrational modes. The region of anomalous damping is marked by the blue stripe. It can clearly be seen that the dissipated energy does not reach the high frequency background modes until the end of the period of anomalous dissipation (Color figure online).

conditions—as illustrated by the inset plot Figure 1(c). In the simple linear damping model, partitioning the system with differing initial excitations would mean that the cooling profiles would all follow portions of the same universal master cooling curve. By plotting the cooling curve of the simulations shifted in time so that starting points of subsequent cooling begin on the cooling profile of other simulations with larger initial

excitations, this point becomes abundantly clear. Rather than tracking the same universal cooling, the trajectories diverge immediately.

The plot in Figure 1(e) shows the attenuation of a single set of simulations [with T_{bg} = 5 K (−268 °C), and T_{ex} = 150 K (−123 °C)] in combination with the Q factor during ring-down. It is observed that the Q factor drops from nearly 2000 by more than 95 pct to ~50 during the period labeled "anomalous dissipation," and then is observed to recover to ~1000 after 40 ps. A more detailed description of the anomalous behavior a previous work[20] (although a slightly different definition of Q factor was used in that work).

Using a projection algorithm,[16] we can determine the energy in any of the CNTs vibrational modes at any time during the simulation; and thus, we can track how the energy populates the background modes once it has been dissipated from the flexural mode. The evolution of this background population is shown in Figure 1(f). It can be observed clearly that the energy goes first into low-frequency modes—close to the frequency of the flexural mode—before dispersing across the full vibrational spectrum of the CNT. The mechanism that causes the nonuniform distribution of background energy is described elsewhere[20] and is caused by a small set of key "gateway modes" that act as strongly nonlinear channels for dissipation. Independent from the details of the mechanism, the athermal distribution of energy in the background modes provides a hidden variable, which is a necessary ingredient for Mpemba-like behavior.

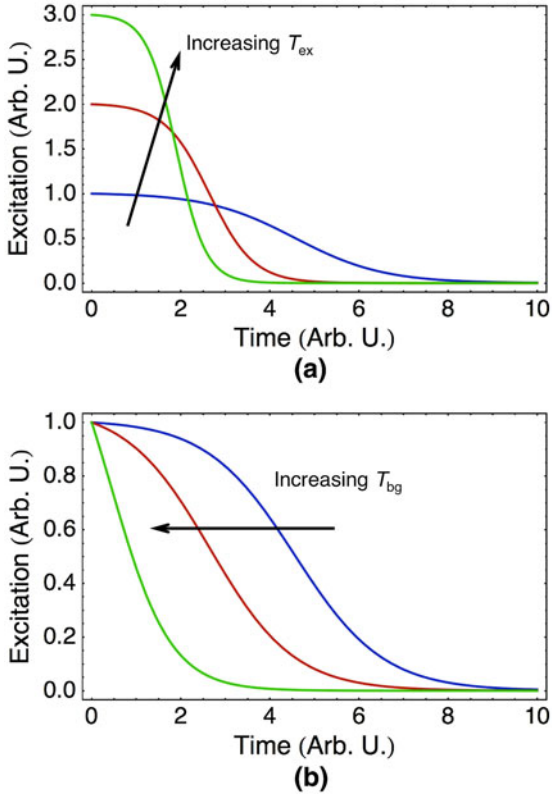

Fig. 2—Attenuation profile for a damped harmonic oscillator with a temperature-dependent damping term (Eq. [2]). Plots (*a*) and (*b*) shows the effects of independently increasing T_{ex}, and T_{bg} respectively.

IV. DISCUSSION

To interpret the attenuation profiles in Figures 1(a) through (c) and (e), it is instructive to consider the attenuation of a simple damped harmonic oscillator with temperature-dependent dissipation. The equation of motion for such an oscillator is given by

$$\ddot{u} = -\omega^2 u - B(T_{bg})\dot{u} \qquad [1]$$

where u, ω, and B, are respectively, the oscillator's displacement, (undamped) frequency, and mass-weighted drag coefficient, with the over-dot indicating the derivative with respect to time. If the period of oscillation is short in comparison with the attenuation time ($\omega \gg B/2$), then we may ignore the oscillatory behavior, noting instead that the rate at which energy is lost to drag is proportional to twice the kinetic energy, and thus the total energy in the oscillator decays according to

$$\dot{E}(t) = -B(T_{bg})E(t) \qquad [2]$$

As a first approximation, the drag term is assumed to take the form of a first-order Taylor expansion: $B(T_{bg}) = B_o + B'\Delta T_{bg}$, with B' positive. The increase in background temperature is simply the energy lost from the oscillator divided by C, the specific heat of the background, so that $\Delta T_{bg} = (E_o - E(t))/C$. Solving Eq. [2] gives the attenuation profile

$$E(t) = E_o \frac{B_f}{B_f - B_i(1 - e^{B_f t})} \qquad [3]$$

(plotted in Figure 2) where $B_i = B_0$ is the initial damping coefficient, and $B_f = B_o + B'E_o/C$ is the damping coefficient when the system is fully relaxed. This simple model displays many features of the molecular dynamics simulations. The attenuation displays an inflection point at a time $t^* = \frac{1}{B_f}\log\left[\frac{B_f}{B_i} - 1\right]$ if the damping coefficient more than doubles as the system relaxes. Increasiing the initial excitation energy E_o increases B_f reducing the total ring-down time (and in effect raising the average dissipation), whereas increasing the initial background energy for the same E_o has the effect of adding an amount ΔB to both B_i and B_f moving the region of steepest attenuation to earlier times.

As can be observed in Figures 2(a) and (b), this simplest model captures many features of the simulated CNT ring-down, including the inflection in the attenuation profile, as well as the trends that arise from independently increasing T_{ex} or T_{bg}. However, the model does not exhibit the Mpemba-like behavior that is observed in CNTs (Figure 1(c)). Decreasing the initial T_{ex}/T_{bg} ratio in the model has the effect of starting the attenuation from further along the same ring-down profile, and thus increasing the initial distance from equilibrium always results in greater cooling time.

The simple model fails to capture several other features of the CNT damping curves in Figures 1(a) through (c) and (e), which hold important clues as to the origin of the Mpemba-like behavior. The model fails to predict the anomalous dissipation region and the recovery of the Q factor: Instead, it predicts Q to decrease monotonically. Related to this is that the tails of the ring-down curves in Figures 1(a) through (c) and (e) flatten out at an energy that is well above its fully relaxed equilibrium value, whereas the tails in Figure 2 decay to zero.

That the tails of the model decay to zero is in itself unphysical. One can develop a slightly different, and phenomenological, model that does equilibriate correctly as follows:

$$\dot{E}(t) = -B(T_{bg})\left(\frac{T_{ex}}{C_{ex}} - \frac{T_{bg}}{C_{bg}}\right)(C_{ex} + C_{bg}), \qquad [4]$$

where C_{ex} and C_{bg} are the specific heat of the excited mode and the set of background modes. The quantities $T_{ex}(C_{ex} + C_{bg})/C_{ex}$, and $T_{bg}(C_{ex} + C_{bg})/C_{bg}$ represent the temperature (that is, the locally time-averaged kinetic energy) of the excited mode and the average temperature of a mode within the background reservoir. Note that this differs from T_{ex} and T_{bg} which were defined to represent the heat in the sets of modes in terms of their contribution to the temperature of the system as a whole. The equation of motion in Eq. [4] can be solved analytically, although it is algebraically messier than Eq. [3], and so the solution is not given here. It displays the same features as Eq. [3] with the exception that in its relaxed state $T_{ex}C_{bg} = T_{bg}C_{ex}$.

The advantage of the phenomenological dissipation model Eq. [4] is that, because the model reaches thermodynamic equilibrium, correctly it can be coupled together into a more complex model that represents the nonlinear cooling of several thermally interacting objects in a closed system. The simplest such case in the context of the CNT dissipation is to divide the background modes into two subsets. One set is the set of modes that interact strongly (and nonlinearly) with the flexural mode, which we call the low-frequency background, and the remainder interact less strongly and are referred to as the high-frequency background. The strongly interacting group is referred to as the low-frequency background because in Figure 1(f), it can be observed that the modes that receive dissipated energy first have in general lower frequencies—although it is important to note that the frequency of the mode is of no importance for this model. The relaxation of this three-body model is now governed by three heat dissipation rates: The power dissipated from the excited mode into the low-frequency background $p_{ex\to l}$, power dissipated from the flexural mode into the high-frequency background $p_{ex\to h}$, and the rate of heat transfer between the low- and high-frequency backgrounds $p_{l\to h}$. The rates p have the form of Eq. [4]. This model is simplified by assuming that the nonlinear term in $p_{ex\to h}$ is zero. This model is solved numerically; as an initial condition, the temperature of the two background sets are the same. It is found that the extra degree of freedom

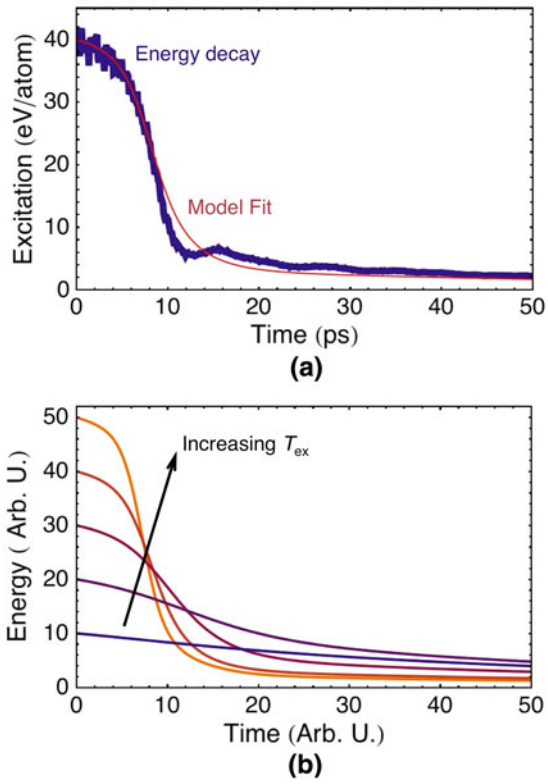

Fig. 3—Attenuation profile predicted by the coupled dissipation model (Eq. [4]). Plot (*a*) shows the model (red) with parameters fit crudely to the simulation data (blue) for a CNT with initial T_{bg} = 100 K (−173 °C), and T_{ex} = 200 K (−73 °C). Plot (*b*) shows the model prediction (with the same fitting parameters) for the simulation data plotted in Fig. 1(c). It is clear that the fit is far from perfect; however, the major features remain. Most importantly, the model reproduces the Mpemba-like behavior (Color figure online).

in the system afforded by the two background reservoirs is sufficient to reproduce all features of the simulated CNT ring-down data—including the observation of Mpemba-like behavior. Figure 3(a) shows the relaxation profile of the model fit to the CNT attenuation profile from Figure 1(e), for which the three linear dissipative terms, one nonlinear dissipative term, and the number of modes in the low frequency background were used as fitting parameters. Figure 3(b) uses the same model parameters as in Figure 3(a) with differing T_{ex}/T_{bg} ratios showing Mpemba-like behavior.

The model plotted in Figures 3(a) and (b) is intended to be illustrative rather than predictive. It shows that two key ingredients are needed to observe the Mpemba-like behavior observed in the CNTs: nonlinear dissipation (caused by heating) and an internal degree of freedom (caused by heterogeneous heating of the background modes). For the fit in Figure 3(a), six fitting parameters were used, which is a lot, and therefore we are reluctant to read too much meaning into them (and have also refrained from fit the model to all of the CNT ring-down data). However, there is one parameter from which we can gain some insight: The number of modes in the low-frequency background. The tail in the ring-down profile occurs when the excited flexural mode

comes into local equilibrium with the low-frequency background, and the initial height of this tail in turn depends on the number of modes the this low-frequency set—that is, the number of modes that interact strongly with the excited flexural mode. To obtain a good fit, we find that this number must be between 3 and 10, which agrees well with our previous finding that a small number of gateway modes trigger rapid dissipation.[20]

V. CONCLUSIONS

The Mpemba effect in the freezing of water is counterintuitive because one assumes that as hot water has cooled down, it passes through the same state as water that is cool initially. This is not the case. The rate of dissipation of heat from the cooling water depends not on the average temperature of the water but on many history-dependent hidden variables, such as the temperature gradient and convective circulation. A comprehensive discussion of the Mpemba effect, its counterintuitive nature, and several competing explanations is given by Jeng.[21] Although the detailed origins of the Mpemba effect in water are not fully agreed on, it is clear that the effect is possible because of internal degrees of freedom within the system that are not described by the average temperature of the system. In this work, it is demonstrated that an abstraction of the same phenomena is possible in other systems such as CNT resonators. The following has been shown in this work:

1. The dissipation results in the formation an athermal populating of vibrational modes that is not described by the average temperature.
2. The dissipative state of the system is extremely sensitive to the athermal phonon population.

These two general results could provide avenues of improving or engineering the properties of real continuously driven CNT resonators. By designing the geometry for maximium heat conduction or by externally heating or cooling specific gateway modes, one could tune the Q factor.

ACKNOWLEDGEMENTS

This project received funding from the Defense Threat Reduction Agency—Joint Science and Technology Office for Chemical and Biological Defense (Grant HDTRA1-09-1-0006).

REFERENCES

1. C. Rutherglen and P. Burke: *Nano Lett*., 2007, vol. 7, pp. 3296–99.
2. K. Jensen, J. Weldon, H. Garcia, and A. Zettl: *Nano Lett*., 2007, vol. 7 (11), pp. 3508–11.
3. J. Weldon, K. Jensen, and A. Zettl: *Phys. Status Solidi B*, 2008, vol. 245, pp. 2323–25.
4. B. Lassagne, D. Garcia-Sanchez, A. Aguasca, and A. Bachtold: *Nano Lett*., 2008, vol. 8, pp. 3735–38.
5. K. Jensen, K. Kim, and A. Zettl: *Nat. Nanotechnol*, 2008, vol. 30, pp. 533–37.
6. A.K. Httell, M. Poot, B. Witkamp, and H. S. J. van der Zant: *New J. Phys*., 2008, vol. 10, p. 095003.
7. V. Sazonova, Y. Yalsh, H. Üstünel, D. Roundy, T.A. Arlas, and P. McEuen: *Nature*, 2004, vol. 431, pp. 284–87.
8. D. Garcia-Sanches, A. San Paulo, M.J. Esplandiu, F. Perez-Murano, L. Forró, A. Aguasca, and A. Bachtold: *Phys. Rev. Lett*., 2007, vol. 99, p. 085501.
9. H.B. Peng, C.W. Chang, S. Aloni, T.D. Yuzvinski, and A. Zettl: *Phys. Rev. Lett*., 2006, vol. 97, p. 087203.
10. B. Witkamp, M. Poot, and H.S.J. van der Zant: *Nano Lett*., 2006, vol. 6, pp. 2904–29–8.
11. A.K. Hüttel, G.A. Steele, B. Witkamp, M. Poot, L.P. Kouwenhoven, and H.S.J. van der Zant: *Nano Lett*., 2009, vol. 9, pp. 2547–52.
12. R. Lifshitz and M. L. Roukes: *Phys. Rev. B*, 2000, vol. 61, pp. 5600–08.
13. K.L. Ekincia and M.L. Roukes: *Rev. Scientif. Instrum*., 2005, vol. 76, p. 061101.
14. K. Jensen, H.B. Peng, and A. Zettl: *Int. Conf. Nanosci. Nanotechnol*., IEEE, New York, NY, 2006, pp. 68–71.
15. H. Jiang, M.-F. Yu, B. Liu, and Y. Huang: *Phys. Rev. Lett*., 2004, vol. 93, p. 185501.
16. P.A. Greaney and J.C. Grossman: *Phys. Rev. Lett*., 2007, vol. 98, p. 125503.
17. S.J. Stuart, A.B. Tutein, and J.A. Harrison: *J. Chem. Phys*., 2000, vol. 112, pp. 6472–86.
18. S. Plimpton: *J. Computat. Phys*., 1995, vol. 117, pp. 1–19. http://lammps.sandia.go.
19. E.B. Mpemba and D.G. Osborne: *Phys. Educ*., 1969, pp. 172–75.
20. P.A. Greaney, G. Lani, G. Cicero, and J.C. Grossman: *Nano Lett*., 2009, vol. 9 (11), pp. 3699–3703.
21. M. Jeng: *Am. J. Phys*., 2006, vol. 74, pp. 514–22.